Seismic Risk Level Screening for Enhanced Geothermal Systems

Wen Zhou[1],
Federica Lanza[2],
Iason Grigoratos[2],
Ryan Schultz[2],
Annemarie Muntendam-Bos[1]

[1] Delft University of Technology, Delft, The Netherlands
[2] Swiss Seismological Service, ETH Zürich, Zürich, Switzerland
[3] University of Geneva, Geneva, Switzerland

Abstract
Induced earthquakes have been in many cases a show-stopper for enhanced geothermal systems (EGS). Thus properly estimating seismic risk prior to investments has significant economic and societal value. Combined with natural geological data, stimulation and operation design, and site vulnerability, we propose a semi-quantitative tool to provide preliminary screening of seismic hazards and risks for the reservoir stimulation for EGS. Applying the screening tool to multiple EGS shows good agreement with project outcomes, which suggest the tool is validated for pre-screening EGS seismic risks.

Introduction
Geothermal, as a sustainable and clean energy, could play an important role in the energy transition to combat global warming. However, conventionally exploited hydro-geothermal energy resources are limited and only accessible in geologically favorable locations.
Deep beneath the surface, temperatures increase significantly, normally with a gradient 25 °C/km. Thus even for areas that aren't in geologically favorable condition, at 3 km depth, temperatures reach around 100°C, making it possible to harness heat by injecting (cold), extracting (hot), and reinjecting (cold) fluids like water. However, low rock porosity and permeability can restrict fluid flow. Enhancing porosity and fluid conductivity can boost geothermal energy production through methods such as hydraulic stimulation or chemical stimulation, resulting in an Enhanced Geothermal System (EGS).
The hydraulic stimulation for EGS, often intentionally targets formations with natural fractures. The escalation of fluid pressure in the reservoir induces slips along fractures, hoping that the slips create dilatation (due to fracture heterogeneity), thus effectively creating pathways in the fracture network. In such a manner, it activates a large portion of a reservoir with limited operations. These induced slips might behave seismically, releasing seismic waves that might be recorded or felt. Induced seismicity is thus an intrinsic nature of EGS.
Additionally, following geothermal productions, there is a decrease in the subsurface temperature which might further induce earthquakes (Parisio et al., 2019; Vörös & Baisch, 2022).

Ideally, we want EGS hydraulic stimulation to generate unfelt microseismicity, e.g., magnitude (ML) < 1, which can help to estimate the dimension of the reservoir and the efficiency of the

stimulation which are important for evaluating economic production. However, large events might occur and pose risks to residents(e.g., noise nuisance, property damages, financial losses and personal safety) and the project operator (e.g., financial losses). For protecting residents and for the sustainability of the EGS projects, it is crucial to quantitatively estimate earthquake risks before the project starts, monitor earthquake activities and re-estimate risks during the projects.

Recent EGS projects in Basel (Deichmann and Giardini, 2009) and Strasbourg (Schmittbuhl et al., 2021) in Europe were terminated due to induced earthquakes of ML 3.4, and ML 3.6, respectively. The EGS project in Pohang, South Korea, caused the largest EGS-related earthquake, registering a magnitude of Mw 5.5 (U.S. Geological Survey; Woo et al., 2019). This earthquake resulted in injuries, property damage, and significant economic damage (Ellsworth et al., 2019; Kim et al., 2018). The failure of these projects, putting a negative impact on the development of EGS projects, but also lessons such as highlighting both the significance of seismic risks and the need for assessment before and during EGS projects.

In the early version of the US protocol for EGS by Major et al. (2012), risk boundary analysis is proposed to classify the project to low to high risk categories. The focus of the risk boundary analysis described by Major et al. (2012) focuses on potential impacts in case of an average expected or worst case seismicity. This approach is useful for regions of sparse population, where a worst case could be possible to be tolerable. If the ‘worst case’ produces intolerable risks, further research and data acquisition could be done to comprehensively characterize the seismic risk and its uncertainty. This is basically the approach taken by Majer et al. (2012). The main uncertainty of this method lies in the estimation of what defines the ‘worst case’ scenario.

Baisch et al., (2016) developed a diagnostic tool, Quick-Scan, for pre-screening seismicity potential in the Netherlands. As part of risk management, the Quick-Scan does not address the perspective of potential impact, which could be justified, given the reality that population density is high in the Netherlands, thus the largest uncertainty lies on the seismicity potential.

For cases in regions of intermediate population density, focusing on only the risk impact or seismicity potential would not provide an effective screening, thus a screening tool that incorporates all components of seismic hazard and risk analysis and public attitude, GRID, is developed by Trutnevyte & Wiemer (2017).

Since 2017, data from negative cases such as the Pohang EGS, GEOVEN deep geothermal (Strasbourg), and positive from Helsinki, FORGE and Blue Mountain, which encourages us to redesign the GRID parameters to incorporate more fault-related parameters into the screening process. It has also become apparent that the impact of water injection operations on induced seismicity varies from region to region. Regional variations in earthquake impacts further necessitate re-evaluation. The GRID or Quick-Scan fall short in addressing these complexities.

Consequently, we have developed a novel diagnostic tool known as Enhanced Geothermal Seismic Risk Screening (EGRS). EGRS is meticulously designed to be as comprehensive and unambiguous as possible, aimed at providing a reliable seismic risk screening for EGS hydraulic stimulation operations. The focus of the framework is hydraulic stimulation, which is a crucial

component of hot-dry-rock EGS. EGRS takes the same approach as GRID, while adopting more comprehensive geological and operational factors and addressing risk directly instead of concern. It is also generalized enough to be easily adapted to new regions.

Overview of the Enhanced Geothermal Seismic Risk Screening (EGRS)

The EGRS is designed to be completed to provide a level of risk concern on seismic hazard and exposure, for EGS projects in any geological context, for the stimulation phase of EGS.
The seismic source, energy propagation, and surface exposure are the most important assets, following the perspective of seismic risk analysis. The seismic source in our case is the size and distribution of induced seismicity, which is controlled by the local geology conditions and the fluid injection operations. The surface exposed assets and their vulnerability is another crucial factor. The subsurface structure can be of important role, and it is the main cause of heterogeneous surface ground motion, but it is secondary in the risk pre-screening.

Thus, we contribute the main control parameters of the EGRA as: (1) the Fault and Geology seismic hazard potential index, (2) the operation seismic hazard potential index, (3) the seismic exposure index.

Firstly, we define the overall seismic risk potential (R) of hydraulic stimulation of the EGRS from the three risk factors: the geology (r_G), the stimulation (r_S), the seismic exposure (r_E),

$$R = \frac{1}{2}(r_G + r_S) \cdot r_E \quad (1)$$

Here the average of geological and stimulation factors indicates the potential of inducing earthquakes. The exposure factor is multiplied with the seismic potential to produce the total risk. It is acknowledged that both geological and operational (stimulation and production) factors play crucial roles in determining the overall earthquake hazard, as they are interrelated (Kraft et al., 2020). By considering them separately as by Walters et al. (2015) and Baisch et al. (2016), the distinct impact on risk assessment can be highlighted. For example: if the fault and geological factors are green, seismicity would be expected to be less likely to occur and the other parameters would also be weighted down. The multiplication in Eq.(1) is justified by the factor that the induced seismicity and the exposed assets must be existing at the same time to pose a risk.

Considering the fact that the data quality (r_Q) can influence the assessment, a penalty to the risk can be added to avoid overconfidence:

$$R = \frac{1}{2}(r_G + r_S) \cdot r_E + (1 - r_Q) \quad (2)$$

The data quality (r_Q) could vary from 0 to 1, thus R has a maximal value of 2. r_Q approaches to 1, as most of the assignments are based on reliable data. It might be also applicable to include the

management plan (r_M) into the risk matrix, as a good management plan could bring the risk lower:

$$R = \frac{1}{2}(r_G + r_S) \cdot r_E + (1 - r_Q) - c \cdot r_M \quad (3)$$

with r_M varies from 0 to 1, where 0 means seismic mitigation measures just meeting regulatory requirements. While 1 means very high quality measures, including site specific risk estimation, high quality research plan and team, conservative seismic mitigation measures on monitoring and TLS and financial mitigation measures. We recommend the weight c on r_M to be 0.2 so that it remains attractive for operators to pursue but also does not overtake the risk estimation.

An overview on applying the Eq. 2 for a risk screening is presented in Table 1.

Table 1. Enhanced Geothermal Seismic Risk Screening (EGRS), scores are assigned based on the Basel Dry-Hot-Rock project.

Risk Parameters				Score
Geological factors (G)				**0.90**
Smallest distance to geologically known active or potentially-active faults [km]				0.67
Earthquake activities				0.90
Smallest distance to any mapped inactive fault [km]				1.00
mapped faults' triggering potential (orientation with active faults)				0.50
Fault or mapped fault plane and reservoir intersection				1.00
Longest mapped fault length in the project facility[km]				1.00
Stimulation factors (O)				**1.00**
Depth of stimulation				1.00
Rock type				1.00
Host reservoir original porosity				1.00
Net injection volume per 100 m times Fluid injection (wellhead) pressure				1.00
Seismic Exposure factors (E)				**1.00**
Population exposure				0.71
Economic exposure (ee)				0.50
Critical infrastructure exposure (ce)				0.50
Penalty Parameters				Score
Data Quality penalty (Q)				**1.00**
Seismic images (6)				6.00
stress field (3)				3.00
Geology maps (3)				3.00
Historical seismicity (3)				3.00
Risk score (R)	L (0 - 0.3)	M (0.3 - 0.6)	H (> 0.6)	**0.95**

Geological factors

The Geological factors evaluate the chance of having critically loaded faults in the facility of the project site. The basic principles are: keeping distance with active faults and seeking a less fractured (faulted) environment.

Active or potentially-active faults

Numerous examples have shown that operating geothermal (EGS or hydrothermal) on large faults very likely would cause unwanted induced seismicity (see review by Buijze et. al., 2019). Lesson from Pohang, is that the EGS project was targeting a site 10 km away from a fault with a large extension, with some sections of the fault having hosted earthquakes recently, although the event was 40 km away and the project site was close to a section that did not have recorded events. The reservoir stimulation triggered a seismicity cloud orienting near parallel to that active fault, suggesting a subfault of the major fault is activated. which means we should not only avoid stimulating an active fault but also keeping distance with it to avoid unknown faults linked to those active faults. GRID (Trutnevyte & Wiemer, 2017) has 'distance to known and potential active fault with a length greater than 3 km'. In GRID, if this distance is larger than 5 km, it considers the concern level is 0. The lesson in Pohang suggests this is underestimating the influence of active faults.
We consider the smallest distance to active or potentially-active faults as an approach to address the its risk concern level.

- < 5 km (1.0)
- 5 - 50 km ($r_{activeF} = 1 - \frac{x-5}{50-5}$)
- > 50 km (0)

Here active and potential active faults are known to have hosted earthquakes or geological studies suggest it might be active. If there is no evidence suggesting a fault in a geology map is in-active, it should be treated as potentially active. Faults, which are mapped from seismic imaging and not known to have hosted earthquakes, are not in this category.

Earthquake activity

It is crucial to keep in mind that geologically known faults are only 'the tip of the iceberg' of faults and fractures of the subsurface. In addition, natural/induced earthquakes could indicate the subsurface is faulted and the unknown faults are active. We consider any seismic activities, whose hosting fault can not be distinguished, to be qualitatively indicators that the region is faulted and the faults are optimal to slip. statistical analysis by Pawley et al. (2018) also suggest natural seismicity rate is a good indicator of induced seismicity activity among shale hydraulic fracturing wells.
Quick-Scan (Baisch et al. 2016) has 'epicentral distance to natural earthquakes' and 'epicentral distance to induced seismicity', with the highest risk concern for distances smaller than 1 km and no concern for larger than 10 km. But it is reasonable to assume larger magnitude events indicate a larger magnitude of susceptibility and a larger area of the critically stressed crust. For practical reasons, we consider any events with magnitude ML>0.5 as smaller size events are often not detected. Without calibration, we assume any event has an influence larger than 2 km radiation, thus any events within 2 km of radiation from the project site has a high risk concern level.

- Any event within 2 km (1.0)
- Event within a distance of 2 to 50 km ($r_{EQ} = 1 - max(0, \frac{(x-2)*5}{(50-2)*M})$)
- No events within 50 km (0)

Mapped faults

Seismic reflection mapped faults or fractures in the facility of the project also have the potential to be triggered to slip, especially during the well stimulation period where the fluid pressure is escalated. Those inactive faults might be mapped through 2D/3D reflection seismic, or vertical seismic profile (VSP) data. Quick-Scan (Baisch et al. 2016) defined 'distance to fault', where fault means mapped (inactive) fault.

Smallest distance to mapped faults

If those fractures are close to the injection well, it is more likely to interact with the stimulation operation, so the smallest distance is considered. So the smallest distance to those mapped faults is a indicating that pressure perturbation on those faults.

- < 0.3 km (1.0)
- 0.3 - 1.5 km ($r_{inactiveF} = 1 - 0.9\frac{x-0.3}{1.5-0.3}$)
- > 1.5 km (0.1)

Length of the longest mapped fault in the project facility

Length of those faults could influence its capacity to host earthquakes and transmitting pressure to distant faults. Purely from the perspective that longer faults have the potential to host larger earthquakes. Based on empirical scaling relation between rupture length and earthquake magnitude (Zoback & Gorelick, 2012; Stein & Wysession, 2013): a moment magnitude 2 event has rupture length between 0.1 to 0.3 km, and moment magnitude 3 event has a rupture length between 0.3 to 1 km. A rupture longer than 1 km has the potential to host a moment magnitude maximal 4 event. Assuming the worst scenario that the entire fault ruptures during one single earthquake. Length of the longest mapped fault in the project facility (2 km around the well stimulation point):

- > 1 km (1.0)
- 0.1 - 1 km ($r_{reactiveLen} = 0.7\frac{x-0.1}{1-0.1} + 0.3$)
- < 0.1 km (0.3)

Mapped faults' triggering potential (orientation with stress field)

The orientation of a mapped fault in relation to the stress field is a strong indicator of the state of a fault (approaching to slip or not).

- Fault is optimally oriented (1.0)
  - A fault is oriented 30±10 degrees from the maximal principal stress direction.
- Fault is intermittently oriented (0.5)
  - A fault is oriented 0±20 or 40-60 degrees from the maximal principal stress direction.
- Fault is unfavorably oriented (0.2)
  - A fault is oriented 60-90 degrees from the maximal principal stress direction.

When multiple faults are mapped, all of them should be considered separately, and the risk concern level is determined by the highest score of all those faults.

The three principal stress directions are normally two horizontal directions and the vertical direction. Earthquake focal mechanism or fault geometry (offsets) could indicate the region is of normal faulting, reverse faulting or striking-slip faulting. In case of normal faulting, the maximal principal stress direction is the vertical direction. It's the dipping angle of fault compared with the vertical direction that influences slipping potential. For reversal faulting, the maximal

principal stress direction is the shortening horizontal direction. For strike-slip faulting, the maximal principal stress direction is around 30 with the fault wall (horizontal) motion direction.
If no stress data is available, the comparison with active fault can be conducted:

- Fault is optimally oriented (1.0) or, a fault is oriented 0±10 or connected with other faults in the region that have hosted earthquakes.
- Fault is intermittently oriented (0.5) or, a fault is oriented 20 - 60 degrees with other faults that have hosted earthquakes (0.5).
- Fault is unfavorably oriented (0.2) or, all faults are oriented 60-90 degrees with other faults that have hosted earthquakes.

It is recommended to conduct detailed geomechanics modeling to investigate whether those inactive faults or fractures have the potential to be triggered, but this is beyond the scope of the first order initial screening.

Fault or mapped fault plane and reservoir intersection

Faults, in or rooted into the basement, are generally advised to avoid, as they can be large and thus produce large induced earthquakes. If the basement is targeted for EGS activity, the site should be clean from any basement faults. Basement faults which extend to sediment layers are relatively easier to identify from offset on the basement-sediment interface. But faults within the basement could be difficult to see from seismic images, because of the lack of continuous impedance interface in the basement.

- Faults, with root to the basement, are evident within the target-reservoir (1)
- Faults are evident in the basement, NOT in the target-reservoir, but the two might be hydraulically connected (no sealing layer in between) (0.9)
- Faults are evident in the basement, NOT in the target-reservoir, and there is evidence for a sealing formation in between that prevents hydraulic connection (0.5)
- No faults evident in the basement or in the target-reservoir, and there is a sealing layer between the reservoir and the basement (0.2)

Resources

While the detailed information for conducting this screening is given in the national annexes, there are some general advises on information collection for geological setting and geomechanical state parameters:

1. Presence of local faults within the project facility (within at least 50 km radiation from the injection point) and their extensions can be found by collecting geology and fault maps from the national Geological agencies.
2. In situ stress: is tectonic stress (e.g., world stress map) indicating the favor of reactivating mapped faults? If applicable, cross-reference this information from in situ stress measurements.
3. Earthquake history:
   - Collect existing information from catalogs of instrumentally recorded, documented (historic reports and/or paleoseismic fault researches) earthquakes from national earthquake agencies. Note the presence of natural earthquakes indicates the presence of active faults and loading from tectonic stress. Yet, the absence of natural earthquakes does not allow the conclusion that no critically stressed fault exists in the study area.
   - Collect earthquake catalogs related to induced activity in the targeted region. Information on induced seismicity (e.g, depth, focal mechanism, relation with mapped faults, etc.) can

be indicative of the criticality of stressed faults. If anthropogenic earthquake activity results from pressure increases (hydraulic fracturing), this can help estimate the scaling ratio between injection operations and earthquakes.

4. Acquire new data:
   - 2D lines or 3D reflection seismic data: over at least 5 km radiation from the injection point.
   - pilot drilling report: are there mud losses or drilling induced events?
   - well logs: can fractures be seen from well logs?

Stimulation factors

The correlation between stimulation operation and seismicity remains a critical topic of induced seismicity. But already, a few factors are known to be more prone to induce or trigger fault slip events. It contains hydrological properties of the intended reservoir (1) Depth and rock type of the stimulation (2) Net fluid injection volume, which has shown, in the first order, to have a linear, although scattered, relationship with maximum magnitude (McGarr 2014). (3) Fluid injection rate and injection pressure, which create a high-pressure zone in the reservoir around the injection well (Shapiro et al., 2010). (4)Temperature decreases during fluid-circulation (thermal production) cause stress changes in the subsurface due to thermal-elastic effect, which could trigger seismicity (Vörös & Baisch, 2022; Cao et al., 2022). In the stage of stimulation, we assume the temperature influence is small compared with the other factors.

Depth of stimulation

In general, the seismogenic property of the crust is evidently to be correlated with depth (Gischig & Wiemer, 2013), for the condition of increasing differential stress. GRID considers operation at depths deeper than 3 km as high risk, 1 - 2 km as medium and shallower than 1 km as low risk. For EGS, we are likely to operate at the high risk category of the GRID. Quick-Scan does not include depth as a variable.
Recent studies on hydraulic fracture (Pawlay et al. 2018) and wastewater injection (Hincks et al. 2018), point to the proximity to basement rock, instead of absolute depth values. As we are designing a pre-screening tool, it is important to keep the evaluation simple, so we still use the absolute depth as an indicator. But note the threshold value can be modified to fit the application region where the basement depth is shallower or deeper.

- > 3 km, (1)
- 1 – 3 km, ($r_{depth} = \frac{x-1}{3-1}$)
- < 1 km, above basement (0)

Rock type

Seismogenic properties are formation dependent, basement crystal rocks are more likely to host earthquakes then sedimentary rock.

- Basement granite, volcanic rock (1)
- Frictional unstable sedimentary rock (0.8)
- Frictional stable sedimentary rock (0.3)

Host reservoir original porosity

We consider fracture-dominated media to be at higher seismic risk, as the fractures will express high normal stress decrease due to pressure escalation due to hydraulic stimulation or thermal contraction due to heat production.

- Fracture dominated, fault damage zone (1)
- Matrix dominated, e.g. porous sandstone, volcanic rocks (0.3)

Planned hydraulic energy

Hydraulic injection is the direct factor of induced seismicity. In GRID, thresholds for net injection volume and pressure range from 1000 to 10,000 m3 and from 0.1 to 1 MPa, respectively, for low to high risk. The Quick-Scan defines the 'possible for inducing seismicity' in a wider range from 5,000 to 20,000 m3 and 4 to 7 MPa. These thresholds are based on experts' experience but not justified.

Reviewing publicly available EGS projects stimulation data, we find the production of pressure and fluid volume presents a log-linear upper limit relationship, although the case of Pohang is a clear outlier. We manually placed two log-linear lines to cover the upper limit for all sites with and without Pohang. As the Pohang EGS site was close to an active fault, which we propose to avoid. If the screening site is indeed distant from any active faults, we could consider the orange curve for setting the thresholds. If the site is within 50 km distance from any active faults, we advise to consider the red curve for setting the thresholds. Note that in Figure X, the magnitude type is not homogenized with half of the data in Mw and the other half in ML. We thus manually fit the two curves, while slightly overestimating, to allow for an error of ~0.3 in magnitude estimations.

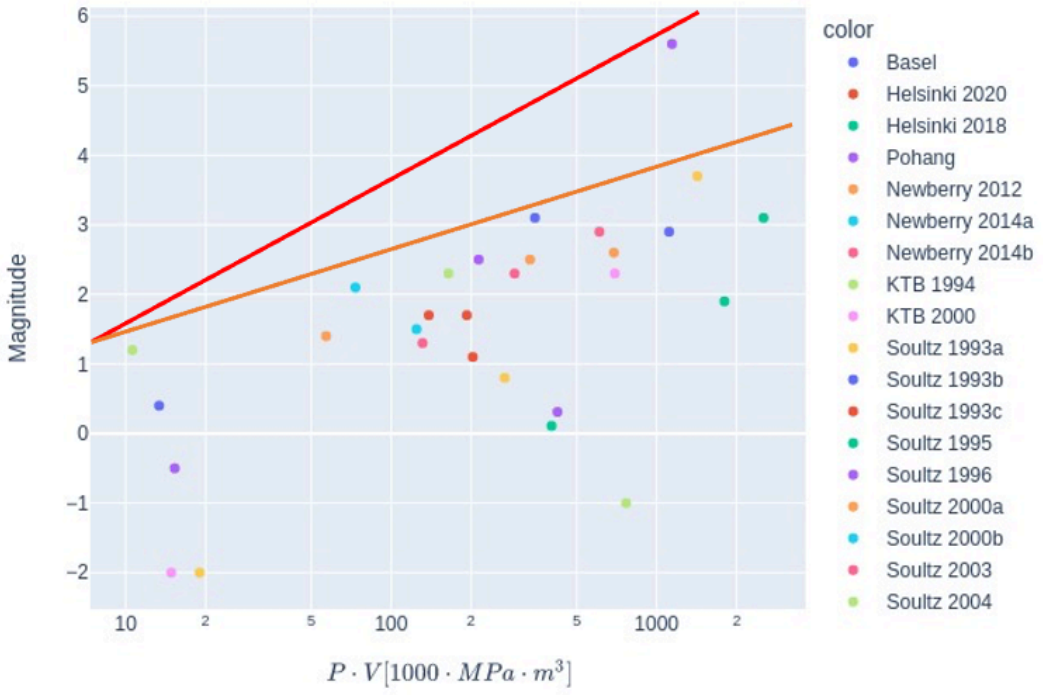

Figure X. maximal induced/triggered earthquake magnitude with their approximated hydraulic energy [net injection volume times maximal wellhead pressure]. Note the magnitude type is not homogenized, with 50% ML and 50% Mw.

For setting the default threshold, we base on the orange curve, and define the highest score based on a magnitude 3 event, which corresponding to $P \cdot V$ around 200 [GPa·m^3], and lowest score on magnitude lower than 1.5 which corresponding to $P \cdot V = 10$ [GPa·m^3].
Recently, we have seen successes on EGS stimulation using multistage stimulation techniques, e.g., Helsinki, FORGE, Blue Mountain. We introduce injection volume per 100 m along the well to distinguish the multi stage injection and the single stage injection. The unit of injection volume per 100 m is based on multistage stimulation which each stage is around 50 m long. We assume the hydraulic connection among every other stage becomes negligible. While this should also be site dependent and should be treated with cautions.
The hydraulic energy [net injection volume (103m3 per 100 m along the well) times maximum wellhead pressure (MPa)]

- High, >200 [$10^3\ MPa\ m^3$] (1.0)
- Median, 10 - 200 [$10^3\ MPa\ m^3$] ($r_{P \cdot V} = \frac{x-10}{200-10}$)
- Low, <10 [$10^3\ MPa\ m^3$] (0)

Seismic Exposure

The impact of induced seismicity on the exposed assets is a crucial part of risk analysis. We suggest the investigation range 10 km for population, critical infrastructures and 50 km for highly critical infrastructures with secondary hazard risk are defined conservatively. If data (ground motion model, source depth distribution model) are available, it might be possible to consider investigating the worst-case scenario earthquakes and define the influence region based on ground motion simulation results. If a worst-case scenario is conducted to investigate the exposure assets, the model selection should be justified and agreed by the independent expert group to conservatively reflect the 'worst-case'.

Exposure assets

- Presence of highly critical infrastructure (e.g. nuclear power plants, dams, oil refineries, cultural heritage sites) within 50 km or of critical infrastructure (e.g. hospitals, noise sensitive laboratories) within 10 km (1.0)
- Dense population with largely non-earthquake-resistant (e.g., Cemented bricks, prefabricated panels without shear load design, clay bricks) buildings within a range of less than 10 km (1.0)
- Dense population with less than 5% non-earthquake-resistant buildings within a range of less than 10 km (0.8)
- Intermediate population density with less than 5% non-earthquake-resistant buildings within 10 km(0.6)
- Sparse population with less than 5% non-earthquake-resistant buildings within 10 km(0.6)
- Sparse population with earthquake-resistant (e.g., wood structure, concrete) buildings within 10 km (0.3)
- Remote area with little to no population within 10 km (0)

The definition of dense or sparse population should be defined by the regulator, based on legislative requirements. In case of no regulation, we suggest a dense population region with

more than 100,000 inhabitants within the 10 km radius, and sparse population as less than 100 inhabitants within the 10 km radius.

Data quality factor

Data quality factor works as a penalty for the hazards and exposure function. If data quality is poor, the operators and other stakeholders are required to acquire the relevant datasets. Data quality is important for every input parameter of the EGRS scores. Poor data quality indicates large uncertainty on the parameters as well as the assessment of the results.
We emphasize four measurements that are important for multiple aspects in EGRS and thus require quality control:

1. Seismic images (2D, 3D seismic reflection profiles, seismic velocity models); This dataset is crucial for estimating hidden fault existence in local scale. Sometimes this information may be supplemented with offsets from well logs.
2. Geological maps (2D, 3D fault and formation maps); Geological data are often available from mining/drilling authorities or national topographic agencies. This data provides important information on regional scale faults.
3. Stress field (tectonic stress field, regional borehole stress measurements, seismic anisotropy measurements, stress tensors derived from earthquake focal mechanisms); Stress data is also important for estimating fault activity, especially for seismically inactive regions.
4. Historical seismicity (instrument recorded seismicity, historical seismicity from scientific literature or palaeo-seismological studies). This data is often available through the national or regional earthquake agencies.
5. Formation properties (drill cores and well loggings) We had a series of points that were related to capture porosity and permeability.

Table X. Data quality penalty table, where the final score is calculated from dividing the summation of all scores by 15. The highest score is 1, which means the operator has all the data acquired in good quality.

Data Quality penalty (Q)													
	Seismic images (6)			stress field (3)			Geology maps (3)			Historical seismicity (3)			**In average**
score	6			3			3			3			**1.00**
Description	3D high resolution cover entire site	few 2D seismic lines	No seismic survey	Leakoff + minifrac + Extended leakoff	1 data point at 5 km away	No stress data	petrophysical data + tectonic fault map			history earthquakes		No data	
	6	3	0	3	2	0				3	1	0	
Data and quality: (1) Resolution of geological settings, 2D or 3D seismic imaging, seismic velocity model, and fault maps. (2) seismic completeness of historical earthquakes. (3)													
*Note: higher scores indicate better data quality													

Depending on the contribution of the data to EGRS, we assign a weight to each dataset. A larger weight of 6 is put on seismic imaging, as it is critical for mapping pre-existing faults. Stress field and geological maps are assigned a weight of 3, whereas historical seismicity is given a weight of 2, as it is easier to obtain.

An important aspect of data quality is to identify parameters/measurements that need to be improved for site-specific risk assessment.

Screening tool validation

Note that the threshold values used in this be stipulated in a national annex as they will depend on the subsurface conditions, etc.

Discussions

References

Atkinson, G. M. (2015). Ground‐Motion Prediction Equation for Small‐to‐Moderate Events at Short Hypocentral Distances, with Application to Induced‐Seismicity Hazards. *Bulletin of the Seismological Society of America*, *105*, 981–992. https://doi.org/10.1785/0120140142

Atkinson, G. M., Worden, C. B., & Wald, D. J. (2014). Intensity Prediction Equations for North America. *Bulletin of the Seismological Society of America*, *104*, 3084–3093. https://doi.org/10.1785/0120140178

Baisch, S., Koch, C., Stang, H., Pittens, B., Drijver, B., & Buik, N. (2016). *Defining the Framework for Seismic Hazard Assessment in Geothermal Projects V0.1 Technical Report*.

Bommer, J. J. (2012). Challenges of Building Logic Trees for Probabilistic Seismic Hazard Analysis. *Earthquake Spectra*, *28*, 1723–1735. https://doi.org/10.1193/1.4000079

Bommer, J. J., & Crowley, H. (2017). The Purpose and Definition of the Minimum Magnitude Limit in PSHA Calculations. *Seismological Research Letters*, *88*, 1097–1106. https://doi.org/10.1785/0220170015

Bommer, J. J., Crowley, H., & Pinho, R. (2015). A risk-mitigation approach to the management of induced seismicity. *Journal of Seismology*, *19*, 623–646.

https://doi.org/10.1007/s10950-015-9478-z

Chiou, B. S.-J., & Youngs, R. R. (2014). Update of the Chiou and Youngs NGA Model for the Average Horizontal Component of Peak Ground Motion and Response Spectra. *Earthquake Spectra*, *30*, 1117–1153. https://doi.org/10.1193/072813eqs219m

Deichmann, N., & Giardini, D. (2009). Earthquakes Induced by the Stimulation of an Enhanced Geothermal System below Basel (Switzerland). *Seismological Research Letters*, *80*, 784–798. https://doi.org/10.1785/gssrl.80.5.784

Diehl, T., Kraft, T., Kissling, E., & Wiemer, S. (2017). The induced earthquake sequence related to the St. Gallen deep geothermal project (Switzerland): Fault reactivation and fluid interactions imaged by microseismicity. *Journal of Geophysical Research: Solid Earth*, *122*, 7272–7290. https://doi.org/10.1002/2017jb014473

Ellsworth, W. L., Giardini, D., Townend, J., Ge, S., & Shimamoto, T. (2019). Triggering of the Pohang, Korea, Earthquake (Mw 5.5) by Enhanced Geothermal System Stimulation. *Seismological Research Letters*, *90*. https://doi.org/10.1785/0220190102

Foulger, G. R., Wilson, M. P., Gluyas, J. G., Julian, B. R., & Davies, R. J. (2018). Global review of human-induced earthquakes. *Earth-Science Reviews*, *178*, 438–514. https://doi.org/10.1016/j.earscirev.2017.07.008

Galis, M., Ampuero, J. P., Mai, P. M., & Cappa, F. (2017). Induced seismicity provides insight into why earthquake ruptures stop. *Science Advances*, *3*, eaap7528. https://doi.org/10.1126/sciadv.aap7528

Grigorato, I., & Papadopoulos, A. (2022). *Milestone 4.2 - Best practice risk assessment for FORGE*.

Gutenberg, B., & Richter, C. F. (1944). Frequency of earthquakes in California*. *Bulletin of the*

Seismological Society of America, *34*, 185–188. https://doi.org/10.1785/bssa0340040185

Kim, K.-H., Ree, J.-H., Kim, Y., Kim, S., Kang, S. Y., & Seo, W. (2018). Assessing whether the 2017Mw5.4 Pohang earthquake in South Korea was an induced event. *Science*, *360*, 1007–1009. https://doi.org/10.1126/science.aat6081

Kraft, T., Roth, P., & Wiemer, S. (2020). *Good Practice Guide for Managing Induced Seismicity in Deep Geothermal Energy Projects in Switzerland*.

Lu, S.-M. (2018). A global review of enhanced geothermal system (EGS). *Renewable and Sustainable Energy Reviews*, *81*, 2902–2921. https://doi.org/10.1016/j.rser.2017.06.097

Majer, E., Nelson, J., Robertson-Tait, A., Savy, J., & Wong, I. (2012). *Protocol for Addressing Induced Seismicity Associated with Enhanced Geothermal Systems*.

Martins, L., Silva, V., Crowley, H., & Cavalieri, F. (2021). Vulnerability modellers toolkit, an open-source platform for vulnerability analysis. *Bulletin of Earthquake Engineering*, *19*, 5691–5709. https://doi.org/10.1007/s10518-021-01187-w

Maxwell, S. C., Rutledge, J., Jones, R., & Fehler, M. (2010). Petroleum reservoir characterization using downhole microseismic monitoring. *GEOPHYSICS*, *75*, 75A129-75A137. https://doi.org/10.1190/1.3477966

McGarr, A. (2014). Maximum magnitude earthquakes induced by fluid injection. *Journal of Geophysical Research: Solid Earth*, *119*, 1008–1019. https://doi.org/10.1002/2013jb010597

Moore, J. (2020). *The Utah FORGE: An International Laboratory for Advancing Enhanced Geothermal Development*.

Moore, J., McLennan, J., Allis, R., Pankow, K., Simmons, S., Podgorney, R., Wannamaker, P., Bartley, J., Jones, C., & Rickard, W. (2019). *The Utah Frontier Observatory for Research*

in Geothermal Energy (FORGE): an International Laboratory for Enhanced Geothermal System Technology Development. https://pangea.stanford.edu/ERE/pdf/IGAstandard/SGW/2019/Moore.pdf

Nievas, C. I., Bommer, J. J., Crowley, H., & van Elk, J. (2019). Global occurrence and impact of small-to-medium magnitude earthquakes: a statistical analysis. *Bulletin of Earthquake Engineering*, *18*, 1–35. https://doi.org/10.1007/s10518-019-00718-w

Parisio, F., Vilarrasa, V., Wang, W., Kolditz, O., & Nagel, T. (2019). The risks of long-term re-injection in supercritical geothermal systems. *Nature Communications*, *10*. https://doi.org/10.1038/s41467-019-12146-0

Schmittbuhl, J., Lambotte, S., Lengliné, O., Grunberg, M., Jund, H., Vergne, J., Cornet, F., Doubre, C., & Masson, F. (2022). Induced and triggered seismicity below the city of Strasbourg, France from November 2019 to January 2021. *Comptes Rendus. Géoscience*, *353*, 561–584. https://doi.org/10.5802/crgeos.71

Schultz, R., Atkinson, G., Eaton, D. W., Gu, Y. J., & Kao, H. (2018). Hydraulic fracturing volume is associated with induced earthquake productivity in the Duvernay play. *Science*, *359*, 304–308. https://doi.org/10.1126/science.aao0159

Schultz, R., Beroza, G. C., & Ellsworth, W. L. (2021a). A risk-based approach for managing hydraulic fracturing–induced seismicity. *Science*, *372*, 504–507. https://doi.org/10.1126/science.abg5451

Schultz, R., Beroza, G. C., & Ellsworth, W. L. (2021b). A Strategy for Choosing Red‐Light Thresholds to Manage Hydraulic Fracturing Induced Seismicity in North America. *Journal of Geophysical Research: Solid Earth*, *126*. https://doi.org/10.1029/2021jb022340

Schultz, R., Ellsworth, W. L., & Beroza, G. C. (2022). Statistical bounds on how induced seismicity stops. *Scientific Reports*, *12*. https://doi.org/10.1038/s41598-022-05216-9

Schultz, R., Muntendam-Bos, A., Zhou, W., Beroza, G. C., & Ellsworth, W. L. (2022). Induced seismicity red-light thresholds for enhanced geothermal prospects in the Netherlands. *Geothermics*, *106*, 102580. https://doi.org/10.1016/j.geothermics.2022.102580

Shapiro, S. A. (2018). Seismogenic Index of Underground Fluid Injections and Productions. *Journal of Geophysical Research: Solid Earth*, *123*, 7983–7997. https://doi.org/10.1029/2018jb015850

Shapiro, S. A., Dinske, C., Langenbruch, C., & Wenzel, F. (2010). Seismogenic index and magnitude probability of earthquakes induced during reservoir fluid stimulations. *The Leading Edge*, *29*, 304–309. https://doi.org/10.1190/1.3353727

Shapiro, S. A., Krüger, O. S., & Dinske, C. (2013). Probability of inducing given-magnitude earthquakes by perturbing finite volumes of rocks. *Journal of Geophysical Research: Solid Earth*, *118*, 3557–3575. https://doi.org/10.1002/jgrb.50264

Trutnevyte, E., & Wiemer, S. (2017). Tailor-made risk governance for induced seismicity of geothermal energy projects: An application to Switzerland. *Geothermics*, *65*, 295–312. https://doi.org/10.1016/j.geothermics.2016.10.006

van der Elst, N. J., Page, M. T., Weiser, D. A., Goebel, T. H. W., & Hosseini, S. M. (2016). Induced earthquake magnitudes are as large as (statistically) expected. *Journal of Geophysical Research: Solid Earth*, *121*, 4575–4590. https://doi.org/10.1002/2016jb012818

van Ginkel, J., Ruigrok, E., Stafleu, J., & Herber, R. (2022). Development of a seismic site-response zonation map for the Netherlands. *Natural Hazards and Earth System*

Sciences, *22*, 41–63. https://doi.org/10.5194/nhess-22-41-2022

Verdon, J. P., & Bommer, J. J. (2020). Green, yellow, red, or out of the blue? An assessment of Traffic Light Schemes to mitigate the impact of hydraulic fracturing-induced seismicity. *Journal of Seismology*, *25*, 301–326. https://doi.org/10.1007/s10950-020-09966-9

Vörös, R., & Baisch, S. (2022). Induced seismicity and seismic risk management – a showcase from the Californië geothermal field (the Netherlands). *Netherlands Journal of Geosciences*, *101*. https://doi.org/10.1017/njg.2022.12

Walters, R. J., Zoback, M. D., Baker, J. W., & Beroza, G. C. (2015). *Version 1 -‐ Spring 2015 Scientific Principles Affecting Protocols for Site-‐characterization and Risk Assessment Related to the Potential for Seismicity Triggered by Saltwater Disposal and Hydraulic Fracturing*.

Wannamaker, P. E., Simmons, S. F., Miller, J. J., Hardwick, C. L., Erickson, B. A., Bowman, S. D., Kirby, S. M., Feigl, K. L., & Moore, J. N. (2020). *Geophysical Activities Over the Utah FORGE Site at the Outset of Project Phase 3*. https://pangea.stanford.edu/ERE/pdf/IGAstandard/SGW/2020/Wannamaker.pdf

Wiemer, S., Kraft, T., Trutnevyte, E., & Roth, P. (2017). *"Good Practice" Guide for Managing Induced Seismicity in Deep Geothermal Energy Projects in Switzerland*.

Woo, J. ‐U., Kim, M., Sheen, D. ‐H., Kang, T. ‐S., Rhie, J., Grigoli, F., Ellsworth, W. L., & Giardini, D. (2019). An In‐Depth Seismological Analysis Revealing a Causal Link Between the 2017 Mw 5.5 Pohang Earthquake and EGS Project. *Journal of Geophysical Research: Solid Earth*, *124*, 13060–13078. https://doi.org/10.1029/2019jb018368

Zalachoris, G., & Rathje, E. M. (2019). Ground Motion Model for Small-to-Moderate Earthquakes in Texas, Oklahoma, and Kansas. *Earthquake Spectra*, *35*, 1–20.

https://doi.org/10.1193/022618eqs047m